

N. Upadyayula · H. S. da Silva · M. O. Bohn  
T. R. Rocheford

## Genetic and QTL analysis of maize tassel and ear inflorescence architecture

Received: 31 July 2005 / Accepted: 10 October 2005  
© Springer-Verlag 2005

**Abstract** Maize (*Zea mays* L.) ear inflorescence architecture is directly relevant to grain yield components, and tassel architecture is relevant to hybrid seed production. The objectives of this study were to (1) determine heritabilities and correlations of a comprehensive set of tassel and ear inflorescence architecture traits in a set of (Illinois Low Protein×B73) B73 S<sub>1</sub> families, (2) identify chromosomal positions of QTL affecting tassel and ear architecture, and (3) identify possible candidate genes associated with these QTL. For tassel traits, the number of detected QTL ranged from one to five, and explained between 6.5 and 35.9% of phenotypic variation. For ear traits, the number of detected QTL ranged from one to nine and phenotypic variation explained by those QTL varied between 7.9 and 53.0%. We detected QTL for tassel architecture traits that required calculation of ratios from measured traits. Some of these calculated traits QTL were detected in regions that did not show QTL for the measured traits, suggesting that calculation of ratios may reveal developmentally relevant patterns of tassel architecture. We detected a QTL on chromosome 7 for tassel branch number near the gene *ramosa1* (*ra1*), which is known to control tassel branch number, making *ra1* a candidate gene for tassel branch number. We detected QTL for several traits on chromosomes 6, 8, and 9, where no inflorescence architecture genes have been mapped, thus providing initial information towards new gene discovery for control of inflorescence architecture.

### Introduction

Maize (*Zea mays* L.) F<sub>1</sub> hybrid seed production requires cross pollination. To ensure high quality seed production, the ideal male parent should have a relatively large tassel that sheds copious amounts of pollen over a long period of time. The ideal female parent should have a relatively large ear that produces a large number of kernels and a relatively small tassel so that more energy is directed toward production of kernels. Plant breeders, however, indirectly select smaller tassels, as tassel size, tassel weight, and tassel branch number, which are shown to be negatively associated with grain yield (Lambert and Johnson 1977; Geraldi et al. 1985; Fischer et al. 1987). Tassel weight of Pioneer hybrids decreased by 36% from 1967 to 1991 (Duvick and Cassman 1999). Tassels will eventually become very small and some breeding lines could become hard to maintain and increase for hybrid production, if this trend continued.

The TopCross<sup>®</sup> pollination system, which is used to produce high oil corn, involves growing fields of male sterile, high yielding commercial hybrids with a small percentage of pollinators of extremely high oil concentration in the grain. Thus, it is important that pollinators have a very large tassel shedding pollen for a long period of time. The contrasting needs for different tassel architectures in different contexts prompts a desire to learn more about genetic control of tassel development, and identification of QTL and genes involved in various stages of tassel inflorescence development. More genetic knowledge will better enable directed manipulations of tassel architecture for different uses.

The components of ear inflorescence architecture such as kernel row number, number of kernels per row, and kernel number density are also grain yield components. Previous quantitative genetic studies suggested indirect selection for greater yield that involved selections of some ear traits could be more effective than direct selection for yield itself, because of lower heritability of yield (Robinson et al. 1951). A long-term

Communicated by S. J. Knapp

N. Upadyayula (✉) · H. S. da Silva · M. O. Bohn  
T. R. Rocheford  
Department of Crop Sciences, University of Illinois,  
Urbana, IL, 61801 USA  
E-mail: upadyayu@uiuc.edu  
Tel.: +1-217-2443388  
Fax: +1-217-3339817

divergent selection experiment for ear length in maize was initiated by Hallauer in 1963 and used to study the effect of ear length on grain yield. Response to selection monitored at the 10th (Cortez-Mendoza and Hallauer 1979), 15th (Salazar and Hallauer 1986), and 27th cycle (Lopez-Reynoso and Hallauer 1998), indicated that grain yield did not increase with selection for longer ear length, but yield decreased significantly with selection for shorter ear length. Odhiambo and Compton (1987), summarizing 20 cycles of divergent mass selection for seed size, reported that grain yield did not increase with selection for greater seed size, but grain yield decreased significantly with selection for smaller seed size. Both studies, however, reported significant positive correlations between grain yield and ear length, cob diameter, kernels per row, and kernel rows per ear, suggesting that each of these components contribute to greater yields. Thus, grain yield is a complex trait that includes several ear architectural components, and a thorough knowledge of the genes affecting the various components and their interactions may lead to better modeling of yield. A better knowledge of these genes and their locations can also be useful in introgression of QTL for other traits, such as disease resistance, as more information will help to design strategies to select for recombinants between favorable and unfavorable alleles within initial introgressed segments.

Although mature tassel and ear architectures appear distinct, their underlying organization and development is remarkably similar until flowers are initiated. Therefore, it is not surprising that some genes affect both tassels and ears. Tassel and ear inflorescences are derived from the inflorescence meristem (IM) (see Fig. 1). The shoot apical meristem (SAM) converts into IM, which produces the tassel. Approximately at the same time, the axillary meristem (AM) initiates lateral IM, which gives

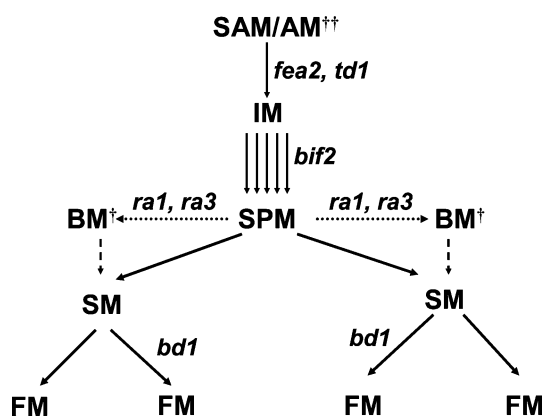


**Fig. 1** Schematic representation of development of tassel and ear inflorescence along with genes likely to affect the various stages of development. <sup>†</sup> BM produced only in tassels. <sup>††</sup> SAM shoot apical meristem, AM axillary meristem, *fea2* fasciated ear2, *td1* thick tassel dwarf1, IM inflorescence meristem, *bif2* barren inflorescence2, SPM spikelet pair meristems, *ra1* ramosa1, *ra3* ramosa3, BM branch meristems, SM spikelet meristems, *bd1* branched silkless1, FM floret meristems

rise to the ear. The IM then initiates secondary and higher order meristems in a progressive manner in both the tassel and the ear (Kaplinsky and Freeling 2003). Each IM produces an indeterminate number of spikelet pair meristems (SPM) in an acropetal and polystichous manner. Each SPM then produce a pair of spikelet meristems (SM), which in turn produces a pair of floret meristems (FM) (Fig. 1). The FM eventually produces the floral organs, the palea/lemma, lodicules, anthers, and pistils. The only difference between the tassel and ear until this point is the first few SPM in the tassel convert into long branch meristems (BM) that produce long branches, while in the ear all SPM convert into a pair of SM and branching is avoided (Kaplinsky and Freeling 2003; Veit et al. 1993). After initiation of the flowers, selective organ abortion in the tassel and ear produces separate unisexual inflorescences. Pistils are aborted in tassels while anthers are aborted in the ear, allowing the tassel and ear to acquire their respective male and female identities (Veit et al. 1993).

A number of mutations are known to affect different steps in the progression from IM to FM, thus defining distinct genetic steps in the development of tassel and ear. *Fasciated ear2* (*fea2*) affects the transition from AM or SAM to IM (see Fig. 1), resulting in the production of a larger IM and thus initiating more branches. SM and FM may also be fasciated, leading to an increase in spikelet production and irregular rows of seeds (Taguchi-Shiobara et al. 2001). *Thick tassel dwarf1* (*td1*) is similar to *fea2*, but it has a pronounced effect on the tassel, resulting in overproduction of spikelets compared to wild type (Bommert et al. 2005a, 2005b). *Barren inflorescence2* (*bif2*) affects the transition from IM to SPM or BM, resulting in the production of fewer ear shoots, branches, spikelets, florets, and floral organs (McSteen and Hake 2001). *Ramosa1* (*ra1*) affects the transition from SPM to BM, resulting in excessive production of branches (Vollbrecht et al. 2005). *Ramosa2* (*ra2*) has a similar effect except that the pedicellate spikelet is converted to a branch. Both *ra1* and *ra2* have a highly branched and distorted ear, suggesting that *ra1* and *ra2* have a role in BM suppression. In ears of *branched silkless1* (*bd1*) mutants, FM are replaced by BM that proliferate SM, suggesting that *bd1* is required for FM identity.

Maize inflorescence architecture is a very amenable system for QTL analysis. Maize inbreds vary considerably for tassel branch number, branching pattern, spikelet density, ear row number, and number of kernels per row. These traits can be measured easily and inexpensively, as well as precisely and accurately, thereby enhancing the power of QTL detection. When the map positioning of a gene, revealed by a maize mutant, correlates with a QTL position, maize mutants affecting inflorescence architecture provide candidate genes for tassel and ear architecture QTL. Conversely if the QTL maps to a region where there are no known, mapped mutants, then it provides initial information for new gene discovery. Therefore, the QTL approach complements efforts to

discover and map genes through the use of mutants stocks, and use of mutants to clone inflorescence genes.

There is considerable literature on ear inflorescence traits in the context of grain yield components (Hallauer et al. 2004; Odhiambo and Compton 1987). In addition, QTL were identified for grain yield components such as cob diameter, ear diameter, number of kernels per row, number of kernels per ear, kernel row number, row length, ear number per plant, and kernel depth (Beavis et al. 1994; Veldboom and Lee 1994; Austin and Lee 1996; Austin et al. 2000). In contrast, limited information has been published on QTL affecting tassel inflorescence architecture. Berke and Rocheford (1999) reported QTL for tassel branch number (TBN), tassel branch angle (TBA), and tassel weight (TW). Mickelson et al. (2002) also reported QTL for TBA and TBN. However, there are many additional traits that comprise tassel architecture besides TBA, TBN, and TW. Traits such as total tassel length, central spike length, branch zone length, spikelet pair density on central spike, spikelet pair density on primary branches, and total spikelets on central spike, are an integral part of tassel architecture. No QTL have been reported for these tassel traits.

The measurement of a comprehensive set of tassel inflorescence architecture traits will help detect the genomic regions that regulate tassel architecture and will help associate some QTL with known mutants affecting tassel architecture. Central spike length is important for calculating the ratios of long BM to SPM and branch zone length to spikelet zone length. This transition from long BM to SPM is relevant to phenotypes associated with maize mutants such as *ral* and *ra2*. Spikelet pair density determines the amount of pollen produced and is relevant to phenotypes similar to *tdl*, *fea2*, *bif2*, and *bal*. Tassel branch length and spikelet pair density on the lowest branch are relevant to variation in the extent of total spikelet coverage of long branches. Variation in branch angle is important, as it determines the area the pollen can be dispersed and also plays a role in shading of the flag leaf. This type of variation is associated with *ra2*. Thus, when QTL for various inflorescence architecture traits map near these genes, they become logical candidate genes underlying the QTL (Robertson 1985).

The objectives of this research were to (1) determine heritabilities and correlations of a comprehensive set of tassel and ear inflorescence architecture traits in a set of (Illinois Low Protein × B73) B73 S<sub>1</sub> families, (2) identify chromosomal positions of QTL affecting tassel and ear architecture, and (3) identify possible candidate genes associated with these QTL.

---

## Materials and methods

### Genetic materials

The corn inbred B73 was crossed to a random single plant of Illinois Low Protein cycle 90 (hereafter referred

to as ILP). A single random F<sub>1</sub> plant was then backcrossed with B73 to generate one ear of BC<sub>1</sub> seed. Plants from the BC<sub>1</sub> generation were self pollinated to generate 150 BC<sub>1</sub>S<sub>1</sub> families. Plants within these families were sibmated to produce enough seed for replicated field evaluation.

### Field evaluation

The 150 BC<sub>1</sub>S<sub>1</sub> families along with five checks, which included the parents, were grown in two replicates in 2003 and 2004 at the University of Illinois Research and Education Center in Urbana, Illinois. Each replicate was randomized as a 31×5 alpha (0,1) design. Measurements were made on five random tassels and five random ears per plot. Tassels were harvested 2 weeks after anthesis and dried in a forced-air drier at approximately 60°C. Eight measurements were taken on the tassels. From these measurements, eight additional characteristics were calculated (see Fig. 2). Five measurements were taken on the cobs. Measurements made on tassels and cobs are listed in Table 1.

### DNA isolation

DNA was isolated from 2-week-old seedling tissues grown from 25 to 30 seeds bulks of each of the 150 BC<sub>1</sub>S<sub>1</sub> families and the parents. Fresh tissue CTAB protocol developed by Mikkilineni (1997) was used to isolate DNA.

### Genotypic data collection

The parents ILP and B73 and six random BC<sub>1</sub>S<sub>1</sub> families were screened with 798 SSR markers from the Maize GDB Public SSR set (2004). Of the markers screened, 120 were found polymorphic. The polymorphic markers were then assayed on the whole population. An aliquot of DNA from 150 BC<sub>1</sub>S<sub>1</sub> families were placed into 96 well plates and diluted 1:25 with water to serve as a template. The PCR protocol used was a modification of the established procedures (Senior et al. 1996). All reactions were run with a PTC-100 with 96 V-bottom well thermocycler (MJ Research, Waltham, MA, USA).

Reaction products were separated by gel electrophoresis in 4% (w/v) metaphor agarose stained with ethidium bromide at 130 V for approximately 2–4 h. Use of Owl gel rigs with five 50-well combs allowed for all progeny assayed with each individual marker to be separated on the same gel. Each gel included one lane of Invitrogen DNA 100-bp ladder. Gels were viewed by means of a Kodak DC 295 digital camera with an ultra violet light filter attached to a Gateway computer running adobe Photoshop Professional Edition. After pictures were taken, the gels were scored, bands were

**Fig. 2** Pictorial representation of measurements taken on tassel.<sup>†</sup> *CSD* central spike spikelet pair density, *TS* total spikelets on central spike, *PSD* primary branch spikelet pair density, *L1* total tassel length, *L2* central spike length, *L3* branch zone length

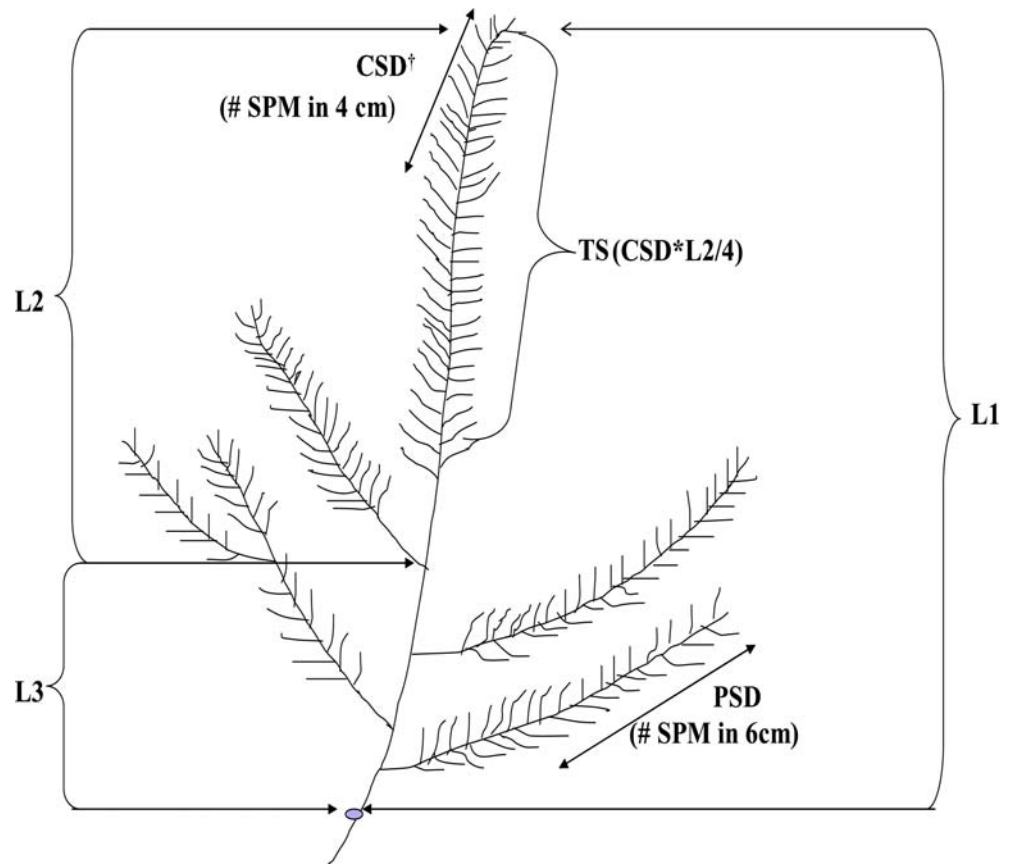


**Table 1** List of tassel and ear inflorescence measurements

Trait	Abbreviation	How measured/calculated
Total tassel length	<i>L1</i>	Measured from the non branching node present below the lowermost primary branch to the tip of central spike
Central spike length	<i>L2</i>	Measured from top branch to tip of central spike
Branch zone length	<i>L3</i>	$L1 - L2$ ; the length from the top branch to the non branching node present below the lowermost primary branch
Branch length	<i>BL</i>	Average length of topmost, lowermost and one random middle primary branch
Tassel weight	<i>TW</i>	Mass in g of entire dried tassel plus 2 cm from the non branching node present below the lowermost primary branch
Tassel branch angle	<i>TBA</i>	Average tassel angle estimated in the field for each family; $0^{\circ}$ = side branches are perpendicular to the central spike, $90^{\circ}$ = side branches are parallel to the central spike
Branch number	<i>BN</i>	Number of primary branches
Central spike spikelet pair density	<i>CSD</i>	Number of spikelet pairs on top 4 cm of central spike
Primary branch spikelet pair density	<i>PSD</i>	Number of spikelet pairs on top 6 cm of lowermost primary branch
Total spikelets on central spike	<i>TS</i>	$(\text{Central spike spikelet pair density} \times \text{central spike length}) / 4$ cm
Branch number/central spike length	$BN/L2$	Ratio of branch number to central spike length
Total spikelets on central spike/branch number	$TS/BN$	Ratio of total spikelets on central spike to branch number
Branch zone length/central spike length	$L3/L2$	Ratio of branch zone length to central spike length
Branch zone length/total tassel length	$L3/L1$	Ratio of branch zone length to total tassel length
Central spike length/total tassel length	$L2/L1$	Ratio of central spike length to total tassel length
Number of kernels/row	<i>KN</i>	Average of number of kernels in two rows on opposite sides of cob
Kernel number density	<i>KD</i>	Average number of kernels per 5 cm in the middle of the two rows used in the above measurement
Number of kernel rows	<i>RN</i>	Number of rows per cob at a height of 5 cm from the shank
Cob diameter	<i>CD</i>	Diameter of the cob in cm at a height of 5 cm from the shank
Cob weight	<i>CW</i>	Total biomass accumulation in the cob in g

scored as “B” for homozygous B73, and “H” for heterozygote of B73/ILP. Restriction fragment length polymorphisms (RFLPs) were identified among the 150 BC<sub>1</sub>S<sub>1</sub> families by following the procedures described by Goldman et al. (1993) and Berke and Rocheford (1995).

Sequence cleaved amplified regions of genes *ral* and *tdl* were mapped using a separate PCR protocol. For *ral*, the initial denaturing was done at 94°C for 90 and 20 s. Annealing temperature was a gradient from 61 to 66°C for 30 s and elongation was done at 70°C for 70 s. This was repeated 34 times. The PCR product was then digested with the DraI enzyme for 2 h at 37°C. Next, the enzyme treated product was run again using the above mentioned PCR protocol. For *tdl*, initial denaturing was done at 95°C for 3 and 1 min. Annealing was done at 53°C for 1 min and elongation was done at 72°C for 2 min. This was repeated 34 times. The PCR product was digested with the SacII enzyme for 2 h at 37°C. The enzyme treated product was run again on agarose gel using the above protocol.

### Genetic linkage map

JoinMap Version 3.0 (Van Ooijen and Voorrips 2001) was used to construct a linkage map for the molecular markers used. JoinMap data analysis tools were used to evaluate quality of molecular marker data. Data were screened for missing data points, segregation distortion, and similarity between markers or individuals. Markers were removed for high level of segregation distortion and missing values. Initial linkage grouping of markers was done at a LOD threshold of 5.5. Groups were joined together based on previous mapping information for these markers (MaizeGDB 2004). The final map included 112 markers (72 SSRs and 40 RFLPs) out of 170 markers (120 SSRs and 50 RFLPs) assayed on the entire population (see Fig. 3). The final map had a total genome length of 1,146 cM and an average interval length of 11.2 cM between markers.

### Phenotypic data analysis

Plot means, range of means, and standard errors were calculated for individual years on the complete unadjusted data set, keeping the replications separate. The plot means for each year were adjusted for  $\alpha$  (0,1) using the mixed procedure (Federer and Wolfinger 1998). The model used for conducting the analysis of variance for all the traits was:

$$y = \mu + \alpha_i + \beta_{j(i)} + \delta_{k(ij)} + \Gamma_l + (\Gamma\alpha)_{il} + \varepsilon_{(ijkl)m} + \phi_{(ijl)n},$$

where  $y$  represents the phenotypic mean for a particular trait of a genotype,  $\alpha$  is the effect of  $i$ th year,  $\beta$  is the effect of  $j$ th replication in the  $i$ th year,  $\delta$  is the effect of  $k$ th block in  $j$ th replication of  $i$ th year,  $\Gamma$  is the effect of

the  $l$ th genotype,  $\Gamma\alpha$  is the effect of  $l$ th family by  $i$ th year interaction, and  $\varepsilon$  represents residual error. Since values were taken on five random plants per family per replication, plants were also included in the model as subsample to get a better estimate of mean, and represented in the model by  $\phi$ . All the effects in the model were considered random. The adjusted means from each year were pooled together to get a grand adjusted mean across years, which was used in the QTL analysis. Estimates of variance components  $\sigma^2$  (error variance),  $\sigma_{ge}^2$  (genotype  $\times$  environment interaction variance), and  $\sigma_g^2$  (genetic variance) of the BC<sub>1</sub>S<sub>1</sub>families were calculated as described by Searle (1971, p 475). Heritabilities ( $\hat{h}^2$ ) for the BC<sub>1</sub>S<sub>1</sub>families were calculated on an entry-mean basis as described by Hallauer and Miranda (1988):

$$\hat{h}^2 = \hat{\sigma}_g^2 / (\hat{\sigma}_g^2 + \hat{\sigma}_{ge}^2 / e + \hat{\sigma}^2 / re),$$

where  $r$  represents number of replications and  $e$  represents number of environments. The 90% confidence intervals on  $\hat{h}^2$  were determined according to Knapp et al. (1985). All the analyses were performed using the SAS statistical software package (SAS Institute 2003). Phenotypic ( $\hat{r}_p$ ) and genotypic ( $\hat{r}_g$ ) correlation coefficients were calculated among the traits based on adjusted entry means of BC<sub>1</sub>S<sub>1</sub> families by applying standard procedures (Mode and Robinson 1959) using PLABSTAT (Utz 2001).

### QTL analysis

The method of Composite Interval Mapping (CIM) (Zeng 1994; Jansen and Stam 1994) was employed for detecting QTL and estimating their effects. The model used for QTL detection was:

$$y_j = b_0 + b_i X_{ij} + \sum_{k \neq i, i+1} b_k X_{kj} + \varepsilon_j$$

where  $y_j$  represents the trait value for the individual  $j$ ,  $b_0$  represents the intercept of the model,  $b_i$  represents the genetic effect of the putative QTL located between markers  $i$  and  $i+1$ ,  $X_{ij}$  represents a dummy variable taking 1 for marker genotype AA and 0 for Aa,  $b_k$  represents the partial regression coefficient of the trait value on marker  $k$ ,  $X_{kj}$  represents dummy variable for marker  $k$  and individual  $j$ , taking 1 if the marker has genotype AA and 0 for Aa, and  $\varepsilon_j$  is a residual from the model. Cofactors were selected for each trait by a step-wise regression procedure (Draper and Smith 1981, p 307ff). Final selection was for the model that minimized Akaike's information criterion with penalty = 3.0. Threshold LOD values for each trait were calculated by performing 1,000 permutations (Churchill and Doerge 1994) at a genome-wise significance level of  $\alpha = 0.30$  which corresponds to a comparison-wise significance of  $\alpha' = 0.0026$ . LOD curves were created by scanning every 2 cM of the genome. For testing the presence of digenic

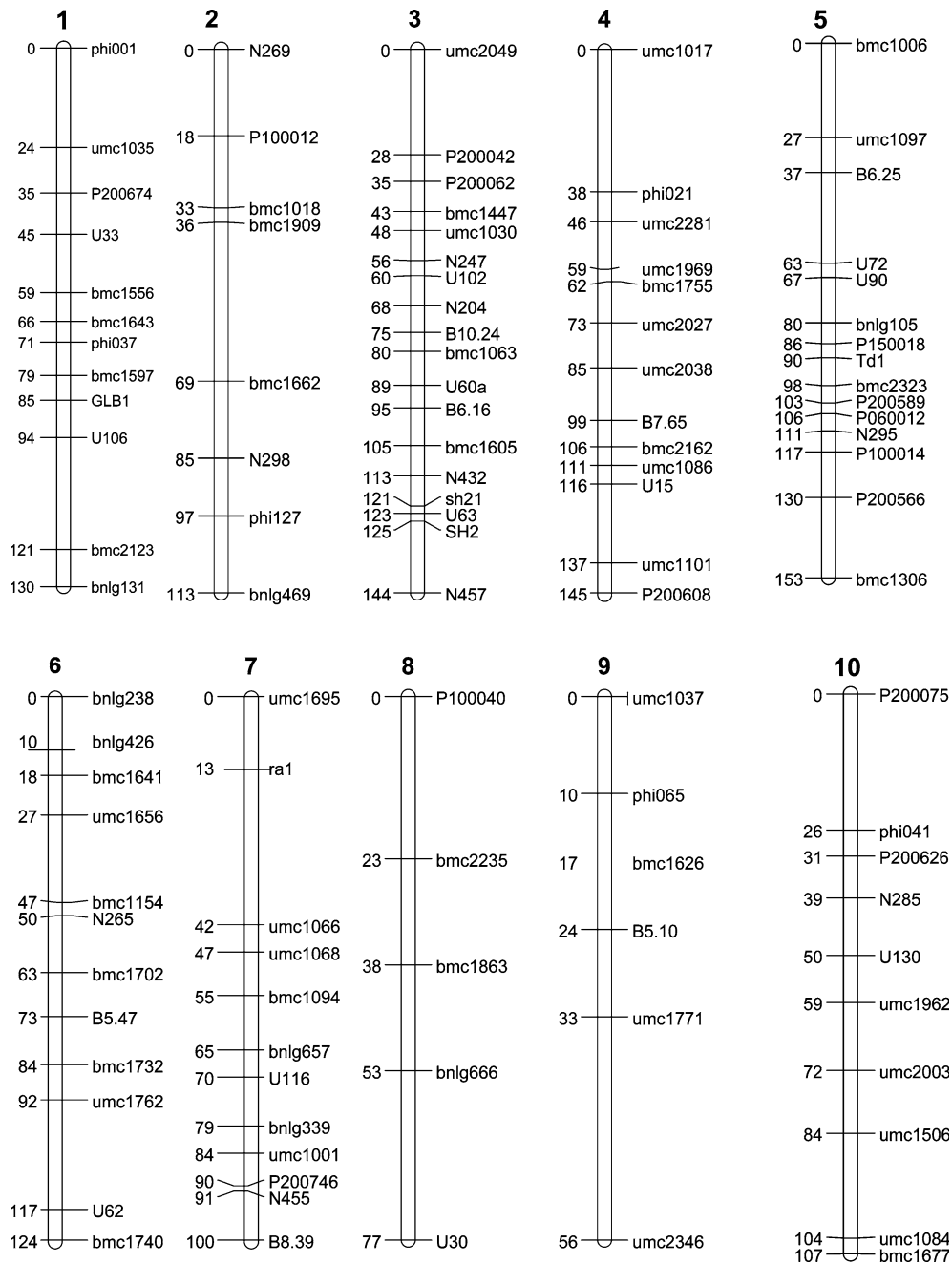


Fig. 3 Molecular map with 72 microsatellite and 40 RFLP positions

epistatic interactions between detected QTL, the regression approach described by Haley and Knott (1992), was adopted. The determination of significant epistatic interaction between detected QTL was based on stepwise regression adding epistatic effects to the main effects in the model by a combination of forward selection and backward elimination. The final choice was for the model that minimized Akaike's information criterion with penalty=3.0. Only those QTL and epistatic interactions that were significant in the final multiple regression model were reported. The phenotypic variation accounted for by an individual QTL ( $R^2$ )

was calculated as the square of the partial correlation coefficient from the final multiple regression model. This value is the coefficient of determination of specified QTL, the phenotypic variation explained by the QTL keeping all the other QTL detected for that trait fixed (Utz and Melchinger 1996). The proportion of phenotypic variance explained by all QTL in the model, with adjustment for the number of terms in the multiple regression models (adjusted  $R^2$ ) was calculated according to Hospital et al. (1997). The percentage of total genotypic variance explained by the model (adjusted  $P$ ) was calculated as adjusted  $R^2$  divided by heritability

(Dudley 1994). QTL for different traits were declared as potential “common QTL,” when they had overlapping confidence intervals.

## Results

### Phenotypic analysis

ILP in comparison with B73 has a larger tassel with more branches (21.5 compared to 7.6), heavier tassel (8.9 g compared to 2.2 g) and denser central spike (33.5 spikelet pairs/4 cm compared to 24.4 spikelet pairs/4 cm), while the central spike length and branch zone length, as well as the ear traits were similar in both parents (Table 2). Analysis of variance across years revealed highly significant ( $P < 0.01$ ) variation among the 150 BC<sub>1</sub>S<sub>1</sub> families for all traits. The family  $\times$  year interactions were not significant for any of the tassel traits or for kernel number. However, interactions were highly significant for kernel number density, cob diameter, row number, and cob weight ( $P < 0.01$ ).

Heritability estimates ( $\hat{h}^2$ ) for directly measured tassel traits ranged from 39% for total tassel length to 83% for tassel weight (Table 2), and for calculated traits  $\hat{h}^2$  ranged from 26% for branch zone length to 73% for branch number/central spike length (Table 2). For kernel number density, cob diameter, and cob weight,  $\sigma_g^2$  estimates were not significantly different from zero.

Branch number was positively correlated with branch zone length ( $r_g = 0.72^{++}$ ), tassel weight ( $r_g = 0.46^{++}$ ), and primary branch spikelet pair density ( $r_g = 0.22^+$ )

(Table 3). Central spike spikelet pair density was positively correlated with primary branch spikelet pair density ( $r_g = 0.63^{++}$ ), central spike length ( $r_g = 0.41^{++}$ ), and total spikelets on central spike ( $r_g = 0.95^{++}$ ). Tassel branch angle showed significant negative correlations with central spike length ( $r_g = -0.46^{++}$ ), primary branch length ( $r_g = -0.40^{++}$ ), spikelet pair density on the central spike ( $r_g = -0.53^{++}$ ), and spikelet pair density on primary branches ( $r_g = -0.45^{++}$ ).

Among ear traits, kernel number per row showed strong positive correlations with kernel row number ( $r_g = 1.00^{++}$ ). Number of kernels per row also showed positive correlations with kernel number density ( $r_p = 0.77^{**}$ ), cob diameter ( $r_p = 0.24^{**}$ ), and cob weight ( $r_p = 0.29^{**}$ ). Kernel row number showed significant positive correlation with cob diameter ( $r_p = 0.42^{**}$ ) and cob weight ( $r_p = 0.27^{**}$ ). However, none of the genotypic correlations for ear traits, except for kernel number per row and kernel row number, were significant.

### Tassel QTL analysis

Four QTL on chromosomes 1, 3, 6, and 7 were found to affect tassel weight (Table 4). A simultaneous fit of all four QTL accounted for a total of 43.2% of  $\hat{\sigma}_g^2$ . The LOD scores ranged from 3.21 in bin 7.03 to 9.66 in bin 1.03. The latter QTL explained 18.7% of  $\hat{\sigma}_g^2$ , whereas the other QTL explained between 4.3 and 15.5% of  $\hat{\sigma}_g^2$ . ILP contributed the allele for heavier tassels for all QTL. Two QTL were detected for tassel branch angle on chromosomes 5 and 9 and explained 25.4% of  $\hat{\sigma}_g^2$ . The

**Table 2** Mean, range and heritability estimates (along with 90% confidence intervals) for tassel and ear traits for 150 S<sub>1</sub> families derived from (ILP  $\times$  B73) B73 along with ILP and B73, combined over years 2003 and 2004

Trait	Units	Mean <sup>a</sup>			Range	$\hat{h}^2$	90% C.I. on $\hat{h}^2$
		ILP	B73	BC <sub>1</sub> S <sub>1</sub>			
Tassel weight	g	8.86 $\pm$ 0.60	2.19 $\pm$ 0.10	3.35 $\pm$ 0.05	2.1–5.4	0.83	(0.77; 0.87)
Cob weight	g	17.56 $\pm$ 1.19	19.57 $\pm$ 0.66	20.27 $\pm$ 0.22	15.2–29.4	NE <sup>b</sup>	NE
Tassel branch angle	degrees	32.36 $\pm$ 1.06	70.00 $\pm$ 1.62	52.45 $\pm$ 0.57	35.0–67.8	0.68	(0.58; 0.76)
Total tassel length	cm	32.29 $\pm$ 0.65	29.80 $\pm$ 0.71	31.97 $\pm$ 0.14	28.3–35.7	0.39	(0.28; 0.58)
Central spike length	cm	21.07 $\pm$ 0.66	21.06 $\pm$ 0.54	23.47 $\pm$ 0.11	20.2–27.2	0.58	(0.46; 0.68)
Branch zone length	cm	11.22 $\pm$ 0.47	8.75 $\pm$ 0.37	8.50 $\pm$ 0.11	5.8–11.7	0.26	(0.06; 0.46)
Primary branch length	cm	18.92 $\pm$ 2.02	14.62 $\pm$ 0.47	16.57 $\pm$ 0.08	14.1–19.6	0.63	(0.55; 0.74)
Cob diameter	cm	2.73 $\pm$ 0.06	2.71 $\pm$ 0.04	2.70 $\pm$ 0.01	2.4–4.0	NE	NE
Branch number	no.	21.50 $\pm$ 1.14	7.60 $\pm$ 0.37	9.85 $\pm$ 0.15	5.7–16.2	0.76	(0.67; 0.81)
Central spike spikelet pair density	no.	33.53 $\pm$ 1.92	24.35 $\pm$ 1.00	26.69 $\pm$ 0.30	18.1–42.5	0.62	(0.51; 0.71)
Primary branch spikelet pair density	no.	21.72 $\pm$ 1.26	10.70 $\pm$ 0.69	14.94 $\pm$ 0.19	10.5–23.2	0.41	(0.23; 0.55)
Total spikelets on central spike	no.	177.37 $\pm$ 12.57	128.66 $\pm$ 6.46	156.95 $\pm$ 2.13	100.1–267.6	0.65	(0.56; 0.75)
Number of kernels/row	no.	21.55 $\pm$ 2.35	23.78 $\pm$ 1.15	23.10 $\pm$ 0.16	17.1–27.8	0.32	(0.21; 0.54)
Row number	no.	14.00 $\pm$ 0.76	16.15 $\pm$ 0.29	14.96 $\pm$ 0.08	12.4–18.6	0.11	(–0.13; 0.34)
Kernel number density	no.	10.36 $\pm$ 0.89	11.63 $\pm$ 0.47	12.14 $\pm$ 0.06	10.2–13.8	NE	NE
Branch number/central spike length	cm <sup>-1</sup>	1.05 $\pm$ 0.10	0.37 $\pm$ 0.02	0.42 $\pm$ 0.01	0.3–0.7	0.73	(0.66; 0.80)
Central spike length/total tassel length		0.65 $\pm$ 0.01	0.71 $\pm$ 0.01	0.73 $\pm$ 0.00 <sup>c</sup>	0.6–0.8	0.52	(0.46; 0.75)
Branch zone length/total tassel length		0.35 $\pm$ 0.01	0.29 $\pm$ 0.01	0.26 $\pm$ 0.00	0.2–0.4	0.52	(0.46; 0.75)
Branch zone length/central spike length		0.54 $\pm$ 0.04	0.42 $\pm$ 0.02	0.36 $\pm$ 0.01	0.2–0.8	0.33	(0.10; 0.48)
Total spikelets on central spike/branch number		8.75 $\pm$ 0.77	17.80 $\pm$ 1.32	16.44 $\pm$ 0.33	8.1–29.3	0.70	(0.62; 0.78)

<sup>a</sup>Standard errors are attached

<sup>b</sup>Not estimable because  $\sigma_g^2$  was 0

<sup>c</sup>Standard error less than 0.01

**Table 3** Phenotypic ( $r_p$ , upper diagonal) and genotypic ( $r_g$ , lower diagonal) correlation coefficients among tassel and ear traits for the 150 S<sub>1</sub> families derived from (ILP × B73) B73 across years 2003 and 2004

Traits	L1	L2	BN	BL	TBA	TW	CSD	PSD	L3	TS	TS/BN	BN/L2	LR	KN	KD	RN	CD	CW
L1 <sup>a</sup>																		
L2	<b>0.80</b> <sup>++</sup>		0.67**	0.44**	-0.23**	0.41**	0.19*	0.10	0.60**	0.39**	0.18*	-0.13	-0.12	-0.14	-0.14	-0.16	-0.04	-0.05
BN	<b>0.19</b> <sup>+</sup>	-0.27 <sup>+</sup>		0.60**	-0.31**	0.32**	0.28**	0.05	-0.20*	0.58**	0.57**	-0.54**	0.62**	-0.09	-0.09	-0.08	-0.02	0.00
BL	<b>0.62</b> <sup>++</sup>	<b>0.73</b> <sup>++</sup>	-0.20 <sup>+</sup>		-0.14	0.43**	0.04	0.16	0.41**	-0.07	-0.70**	0.95**	-0.52**	0.06	-0.03	-0.01	0.04	-0.19*
TBA	-0.44 <sup>+</sup>	-0.46 <sup>+</sup>	-0.15 <sup>+</sup>	-0.40 <sup>+</sup>		0.34**	0.04	0.04	-0.06	0.24**	0.29**	-0.30**	0.27**	-0.05	-0.03	-0.04	0.12	0.20*
TW	<b>0.60</b> <sup>++</sup>	<b>0.39</b> <sup>++</sup>	<b>0.46</b> <sup>++</sup>	<b>0.36</b> <sup>++</sup>	-0.48 <sup>++</sup>		-0.37**	-0.20*	0.02	-0.41**	-0.19*	-0.04	-0.14	-0.11	-0.14	-0.1	-0.24**	0.07
CSD	<b>0.32</b> <sup>+</sup>	<b>0.41</b> <sup>+</sup>	<b>0.01</b>	<b>0.12</b>	-0.53 <sup>++</sup>	<b>0.73</b> <sup>++</sup>		0.49**	0.20*	0.57**	0.09	0.29**	0.00	-0.06	-0.11	-0.03	0.14	-0.05
PSD	-0.01	<b>0.01</b>	<b>0.22</b> <sup>+</sup>	-0.03	-0.45	<b>0.74</b> <sup>++</sup>	<b>0.63</b> <sup>++</sup>	0.40**	-0.05	0.94**	0.61**	-0.05	0.24**	-0.05	-0.12	-0.02	0.04	-0.07
L3	<b>0.40</b> <sup>+</sup>	-0.22 <sup>+</sup>	<b>0.72</b> <sup>++</sup>	-0.11	-0.01	<b>0.39</b> <sup>++</sup>	<b>0.11</b>	0.07	0.07	0.37**	0.15	0.13	0.01	-0.02	0.01	0.05	0.12	-0.11
TS	<b>0.54</b> <sup>++</sup>	<b>0.67</b> <sup>++</sup>	-0.09	<b>0.34</b> <sup>++</sup>	-0.58	<b>0.73</b> <sup>++</sup>	<b>0.95</b> <sup>++</sup>	-0.16	-0.16	-0.12	-0.38**	0.41**	-0.82**	-0.08	-0.08	-0.13	-0.03	-0.06
TS/BN	<b>0.16</b>	<b>0.61</b> <sup>++</sup>	-0.75 <sup>++</sup>	<b>0.39</b> <sup>++</sup>	-0.29	<b>0.17</b>	<b>0.61</b> <sup>++</sup>	<b>0.21</b> <sup>+</sup>	-0.70 <sup>++</sup>	<b>0.70</b> <sup>++</sup>	<b>0.72</b> <sup>++</sup>	-0.23**	0.42**	-0.08	-0.13	-0.04	0.03	-0.05
BN/L2	-0.05	-0.50 <sup>+</sup>	<b>0.97</b> <sup>++</sup>	-0.36 <sup>++</sup>	-0.03	<b>0.32</b> <sup>++</sup>	-0.10	<b>0.20</b> <sup>+</sup>	<b>0.67</b> <sup>++</sup>	-0.25 <sup>++</sup>	-0.82 <sup>++</sup>	-0.77**	0.65**	0.09	0.01	0.03	0.05	-0.16*
LR	<b>0.08</b>	<b>0.66</b> <sup>++</sup>	-0.64 <sup>++</sup>	<b>0.39</b> <sup>++</sup>	-0.20 <sup>+</sup>	-0.01	<b>0.39</b> <sup>++</sup>	<b>0.15</b>	-0.88 <sup>++</sup>	<b>0.54</b> <sup>++</sup>	<b>0.83</b> <sup>++</sup>	-0.73 <sup>++</sup>	-0.64**	0.01	0.02	0.06	0.05	0.01
KN	-0.25	-0.20	<b>0.14</b>	-0.13	-0.27 <sup>+</sup>	-0.09	-0.13	-0.16	-0.11	-0.17 <sup>+</sup>	-0.21 <sup>+</sup>	<b>0.20</b> <sup>+</sup>	-0.05	0.01	0.77**	0.79**	0.24**	0.29**
KD	<b>0.00</b>	<b>0.00</b>	<b>0.00</b>	<b>0.00</b>	<b>0.00</b>	<b>0.00</b>	<b>0.00</b>	<b>0.00</b>	<b>0.00</b>	<b>0.00</b>	<b>0.00</b>	<b>0.00</b>	<b>0.00</b>	<b>0.00</b>	<b>0.00</b>	0.92**	0.39**	0.22**
RN	-0.18	-0.15	-0.01	-0.15	-0.39 <sup>+</sup>	-0.04	-0.18	-0.14	-0.05	-0.20	-0.02	<b>0.08</b>	-0.01	<b>1.00</b> <sup>+</sup>	<b>0.00</b>	<b>0.00</b>	<b>0.42</b> <sup>**</sup>	<b>0.27</b> <sup>**</sup>
CD	<b>0.00</b>	<b>0.00</b>	<b>0.00</b>	<b>0.00</b>	<b>0.00</b>	<b>0.00</b>	<b>0.00</b>	<b>0.00</b>	<b>0.00</b>	<b>0.00</b>	<b>0.00</b>	<b>0.00</b>	<b>0.00</b>	<b>0.00</b>	<b>0.00</b>	<b>0.00</b>	<b>0.00</b>	<b>0.00</b>
CW	<b>0.00</b>	<b>0.00</b>	<b>0.00</b>	<b>0.00</b>	<b>0.00</b>	<b>0.00</b>	<b>0.00</b>	<b>0.00</b>	<b>0.00</b>	<b>0.00</b>	<b>0.00</b>	<b>0.00</b>	<b>0.00</b>	<b>0.00</b>	<b>0.00</b>	<b>0.00</b>	<b>0.00</b>	<b>0.00</b>

<sup>a</sup>Phenotypic correlation was significant at the 0.05 probability level

\*\*Phenotypic correlation was significant at the 0.01 probability level

<sup>+</sup> Genotypic correlation exceeded one time its standard error

<sup>++</sup> Genotypic correlation exceeded two times its standard error

<sup>a</sup>L1 total tassel length, L2 central spike length, BN branch number, BL primary branch length, TBA tassel branch angle, TW tassel weight, CSD central spike spikelet pair density, PSD primary branch spikelet pair density, L3 branch zone length, TS total spikelets on central spike, TS/BN total spikelets on central spike/branch number, BN/L2 branch number/central spike length, LR tassel length ratios, KN kernel number per row, KD kernel number density, RN kernel row number per cob, CD cob diameter, CW cob weight

**Table 4** Parameters associated with QTL for tassel traits (measured), estimated from 150 S<sub>j</sub> families derived from (ILP × B73) B73

Trait	Bin <sup>a</sup>	QTL position <sup>b</sup>	Marker interval	Support interval	LOD	QTL effect <sup>c</sup>	Partial R <sup>2d</sup>
Central spike length	4.05	62	bmc1755–umc2027	58–68	5.28	1.85 cm	13.6
	4.08	112	Umc1086–u15	104–116	2.71	1.30 cm	5.3
	5.06	146	p200566–bmc1306	134–152	3.59	–1.66 cm	6.5
	6.07	118	U62–bmc1740	106–124	4.81	–1.68 cm	14.1
							R <sup>2e</sup> = 26.6%
							P <sup>f</sup> = 45.8%
Branch number	4.05	62	bmc1755–umc2027	58–72	2.92	–1.71 (#)	11.7
	7.00	0	umc1695–ral	0–8	2.75	–1.59 (#)	7.9
							R <sup>2</sup> = 17.8%
							P = 23.4%
Tassel weight	1.03	0	phi001–umc1035	0–8	9.66	–0.95 g	18.7
	3.07	110	bmc1605–n432	102–118	3.37	–0.54 g	4.3
	6.06	116	umc1762–u62	108–122	8.08	–0.88 g	15.5
	7.03	92	n455–b8.39	88–98	3.21	–0.55 g	12.2
							R <sup>2</sup> = 35.9%
							P = 43.2%
Tassel branch angle	5.04	102	bmc2323–p200589	98–106	3.79	7.73°	15.8
	9.02	0	umc1037–phi065	0–2	3.28	5.99°	5.8
							R <sup>2</sup> = 17.3%
							P = 25.4%
Central spike spikelet pair density	1.09	82	bmc1597–glb1	78–88	4.71	5.26 (#)	9.3
	2.08	72	bmc1662–n298	52–84	3.43	–4.04 (#)	9.7
	5.06	152	p200566–bmc1306	140–152	3.11	–3.75 (#)	5.1
	6.07	122	u62–bmc1740	108–124	2.67	–3.50 (#)	10.2
	8.02	36	bmc2235–bmc1863	26–46	3.68	–4.19 (#)	12.1
							R <sup>2</sup> = 26.8%
							P = 43.3%
Primary branch spikelet pair density	5.04	112	n295–p100014	106–118	2.88	–2.30 (#)	8.6
	9.02	8	Umc1037–phi065 [5/112, 9/8] <sup>g</sup>	0–16	2.87	–2.35 (#)	6.6
							2.8
							R <sup>2</sup> = 9.3%
							P = 22.6%

<sup>a</sup>Bin number of left flanking marker, taken from Maize GDB

<sup>b</sup>QTL position in cM from the top of the chromosome as calculated by PLABQTL

<sup>c</sup>The additive effect of each QTL is calculated as (mean of the B73 genotypic class – mean of ILP genotypic class). Therefore, positive values indicate that B73 carries the allele for an increase in the trait, and negative values indicate that ILP contributes the alleles for an increase in the trait

<sup>d</sup>Proportion of phenotypic variation accounted for each QTL calculated by multiple regression in PLABQTL

<sup>e</sup>Proportion of phenotypic variation explained by the final model

<sup>f</sup>Proportion of genotypic variation explained by the final model

<sup>g</sup>Additive by additive epistatic interaction

QTL in bin 5.04 explained 15.8% of  $\hat{\sigma}_p^2$  while the QTL in bin 9.02 accounted for 5.8% of  $\hat{\sigma}_p^2$ . The allele for greater tassel branch angle came from B73 for both QTL. Two QTL accounting for 23.4% of  $\hat{\sigma}_g^2$  were identified for tassel branch number. The QTL in bin 7.00 explained 7.9% of  $\hat{\sigma}_p^2$  and *ral* was the flanking marker, while the other QTL on chromosome 4 explained 11.7% of  $\hat{\sigma}_p^2$ . The allele for higher branch number for both QTL came from ILP. Five QTL explaining a total of 43.3% of  $\hat{\sigma}_g^2$  on chromosomes 1, 2, 5, 6, and 8 were detected for spikelet pair density on central spike. The QTL in bin 8.02 explained 12.1% of  $\hat{\sigma}_p^2$ , whereas the other QTL explained between 5.1 and 10.2% of  $\hat{\sigma}_p^2$ . Two QTL explaining a total of 22.6% of  $\hat{\sigma}_g^2$  were detected for spikelet pair density on primary branches. The QTL in bin 5.04 explained 8.6% of  $\hat{\sigma}_p^2$  while the QTL in bin 9.02 explained 6.6% of  $\hat{\sigma}_p^2$ . The allele for higher spikelet pair density on the branches came from ILP. Both QTL showed significant epistatic interaction and accounted for 2.8% of  $\hat{\sigma}_p^2$ . For branch zone length, a single QTL

was detected, in bin 9.02 (Table 5). A single QTL explaining 24.0% of  $\hat{\sigma}_g^2$  was detected for branch number/central spike length ratio (BN/ L2) in bin 4.05. For branch zone length/central spike length ratio (L3/ L2), branch zone length/total tassel length ratio (L3/ L1) and central spike length/total tassel length ratio (L2/ L1) we detected a single QTL in bin 9.02 and accounted for 19.6, 13.0, and 13.0% of  $\hat{\sigma}_g^2$ , respectively (Table 5).

#### Ear QTL analysis

We detected QTL for all ear traits (Table 6). Nine QTL involved in inheritance of cob weight were identified on chromosomes 1, 2, 3, 4, 5 (two QTL), 6, and 7 (two QTL). The QTL in bin 3.08 explained 21.1% of  $\hat{\sigma}_p^2$  whereas the other QTL explained between 5.6 and 20.5% of  $\hat{\sigma}_p^2$ . A simultaneous fit of all nine QTL accounted for 53% of  $\hat{\sigma}_p^2$ . The QTL model for kernel number per row included four QTL on chromosomes 3 (two QTL), 4, and

**Table 5** Parameters associated with QTL for tassel traits (calculated), estimated from 150 S<sub>1</sub> families derived from (ILP × B73) B73

Trait	Bin <sup>a</sup>	QTL position <sup>b</sup>	Marker interval	Support interval	LOD	QTL effect <sup>c</sup>	Partial R <sup>2d</sup>
Branch zone length	9.02	8	umc1037–phi065	2–14	4.13	0.59 cm	8.1 R <sup>2e</sup> = 7.8% P <sup>f</sup> = 30.2%
Total spikelets on central spike	5.06	152	p200566–bmc1306	136–152	3.20	–25.03 (#)	6.9
	6.07	122	u62–bmc1740	108–124	4.88	–32.60 (#)	10.5
	8.02	36	bmc2235–bmc1863	24–52	2.66	–23.44 (#)	7.3 R <sup>2</sup> = 17.8% P = 27.4%
Total spikelets on central spike/branch number	4.08	106	bmc2162–umc1086	98–112	2.66	3.73	11.3
	8.02	34	bmc2235–bmc1863	28–46	5.62	–5.16	5.7 R <sup>2</sup> = 12.5% P = 17.9%
Branch number/central spike length	4.05	62	bmc1755–umc2027	58–68	4.72	–0.11 cm <sup>–1</sup>	18.4 R <sup>2</sup> = 17.5% P = 24.0%
Branch zone length/central spike length	9.02	8	umc1037–phi065	2–14	4.23	0.09	7.7 R <sup>2</sup> = 6.5% P = 19.6%
Branch zone length/total tassel length	9.02	8	umc1037–phi065	2–16	3.96	0.04	8.0 R <sup>2</sup> = 6.8% P = 13.0%
Central spike length/total tassel length	9.02	8	umc1037–phi065	2–16	3.96	0.04	8.0 R <sup>2</sup> = 6.8% P = 13.0%

<sup>a</sup>Bin number of left flanking marker, taken from Maize GDB

<sup>b</sup>QTL Position in cM from the top of the Chromosome as calculated by PLABQTL

<sup>c</sup>The additive effect of each QTL is calculated as (mean of the B73 genotypic class–mean of ILP genotypic class). Therefore, positive values indicate that B73 carries the allele for an increase in the trait, and negative values indicate that ILP contributes the alleles for an increase in the trait

<sup>d</sup>Proportion of phenotypic variation accounted for each QTL calculated by multiple regression in PLABQTL

<sup>e</sup>Proportion of phenotypic variation explained by the final model

<sup>f</sup>Proportion of genotypic variation explained by the final model

8 and accounted for 20.1% of total  $\hat{\sigma}_p^2$ . A QTL with large effects was detected in bin 3.02, with a LOD score of 6.7 and explained 16.5% of  $\hat{\sigma}_p^2$ . A single QTL explaining 7.9% of  $\hat{\sigma}_p^2$  was detected in bin 2.04 for kernel number density. Two QTL were detected for row number on chromosomes 3 and 10 and explained 10.7% of  $\hat{\sigma}_p^2$ . Two QTL explaining 14.7% of  $\hat{\sigma}_p^2$  on chromosomes 1 and 5 were identified for cob diameter.

### Comparison across traits

Based on confidence intervals, all the QTL were summarized as 24 different QTL (see Fig. 4), 50% of which were common for two or more traits. Among the tassel traits, central spike length and the ratio total spikelets on central spike/branch number shared a common QTL on chromosome 4. Central spike length, spikelet pair density on central spike, and total spikelets on central spike had a common QTL on chromosomes 5 and 6. On chromosome 9, common QTL were detected for tassel branch angle, branch zone length, spikelet pair density on primary branch, and all the tassel length ratios. Three QTL on chromosomes 1, 2, and 4 were common for two ear traits. Common QTL were detected for cob diameter and cob weight on chromosome 1, kernel number density and cob weight on chromosome 2, and kernel row

number and cob weight on chromosome 4. Four out of 25 QTL were common for tassel and ear traits. Kernel row number, tassel weight, and cob weight shared a common QTL on chromosome 3, cob weight, tassel branch angle and spikelet pair density on primary branches had a common QTL on chromosome 5, and on chromosome 7 branch number and cob weight shared a common QTL.

### Discussion

Efficiency of indirect selection depends on (i) the genetic correlation between selected trait and the target trait, and (ii) high heritability of the selected trait (Falconer 1989). We detected significant correlations between different components of tassel architecture, and some may be useful for selecting lines within this type of germplasm as it relates to hybrid production.

The positive correlation between central spike length and total spikelets on central spike ( $r_g = 0.67^{++}$ ), supported by 40% of the QTL detected being in common (see Table 7). This suggests central spike length can be used in the selection for pollen production, as might be expected. We also detected a positive correlation between central spike length and central spike spikelet pair density ( $r_g = 0.41^{++}$ ), which was not expected.

**Table 6** Parameters associated with QTL for ear traits, estimated from 150 S<sub>1</sub> families derived from (ILP × B73) B73

Trait	Bin <sup>a</sup>	QTL position <sup>b</sup>	Marker interval	Support interval	LOD	QTL effect <sup>c</sup>	Partial R <sup>2d</sup>
Kernel number/row	3.02	38	p200042–bmc1447	34–44	6.74	–3.46 (#)	16.5
	3.06	88	u60a–b6.16	82–92	3.22	2.34 (#)	6.8
	4.09	144	umc1101–p200608	138–144	3.86	2.56 (#)	3.9
	8.02	14	p100040–bmc2235	0–28	2.68	–2.18 (#)	5.8
							R <sup>2e</sup> = 20.1%
							P <sup>f</sup> = 62.9%
Kernel number density	2.04	28	p100012–bmc1018	18–36	2.98	0.88 (#)	9.1
							R <sup>2</sup> = 7.9%
Row number/cob	3.07	106	bmc1605–n432	102–118	3.69	1.16 (#)	7.5
	10.01	0	p200075–phi041	0–12	3.09	–1.06 (#)	5.7
							R <sup>2</sup> = 10.7%
Cob diameter	1.07	56	u33–bmc1556	48–64	4.16	–0.21 cm	10.1
	5.02	78	u90–bnlg105	70–84	3.54	0.18 cm	9.1
							R <sup>2</sup> = 14.7%
Cob weight	1.07	62	bmc1556–bmc1643	60–66	5.88	–3.78 g	20.5
	2.04	34	bmc1018–bmc1909	32–48	8.27	–3.47 g	14.3
	3.08	118	n432–sh21	114–122	5.85	3.02 g	21.1
	4.09	144	umc1101–p200608	138–144	3.45	2.42 g	5.6
	5.04	92	td1–bmc2323	88–96	4.67	3.04 g	10.5
	5.04	116	n295–p100014	110–130	2.57	2.15 g	5.6
	6.05	50	bmc1154–n265	34–52	5.07	–2.90 g	8.5
	7.00	12	umc1695–ral	6–14	3.66	2.42 g	11.8
	7.01	44	umc1066–umc1068	42–48	3.91	–2.55 g	10.8
							R <sup>2</sup> = 53.0%

<sup>a</sup>Bin number of left flanking marker, taken from Maize GDB

<sup>b</sup>QTL position in cM from the top of the Chromosome as calculated by PLABQTL

<sup>c</sup>The additive effect of each QTL is calculated as (mean of the B73 genotypic class – mean of ILP genotypic class). Therefore, positive values indicate that B73 carries the allele for an increase in the trait, and negative values indicate that ILP contributes the alleles for an increase in the trait

<sup>d</sup>Proportion of phenotypic variation accounted for each QTL calculated by multiple regression in PLABQTL

<sup>e</sup>Proportion of phenotypic variation explained by the final model

<sup>f</sup>Proportion of genotypic variation explained by the final model

Another trait that might be used for indirect selection is the tassel branch angle. Tassel branch angle showed significant negative correlation with the spikelet pair densities on the central spike ( $r_g = -0.53^{++}$ ) and primary branches ( $r_g = -0.45^{++}$ ). The correlation between TBA and PSD was supported with both the QTL detected for these traits (in bins 5.04 and 9.02) being in common. Assuming pollen dispersal is adequate, upright tassels would also minimize the amount of shading per unit of biomass and enhance light interception (Mickelson et al. 2002). Therefore, altering tassel angle may be a strategy to minimize shading and to improve yields without sacrificing tassel size. These trends, however, need to be confirmed in other populations, and higher  $r_g$  values would be desirable for indirect selection to be more effective.

Among ear traits, kernel number per row and row number showed significant positive correlation ( $r_g = 1.00^{++}$ ), contrary to the findings reported by Hallauer et al. (2004) for the population Iowa Long Ear Synthetic (BSLE). Hallauer et al. (2004) compared cycles C<sub>0</sub>–C<sub>27</sub> of the long-term divergent selection and found ear length and kernel row number varying in opposite direction. One reason for this discrepancy might be that our population was derived from a bipa-

rental cross and involved no selection while BSLE population, developed by intermating 12 inbred lines from different heterotic groups, underwent recurrent selection. Consistent with Hallauer et al. (2004), we did not find significant correlations between other ear traits.

Based on the observation that larger tassel size has been negatively associated with grain yield, we inspected for significant negative correlations between the various tassel and ear architecture components. We found only two low but significant negative correlations, between tassel branch angle and kernel number per row ( $r_g = -0.27^+$ ), and tassel branch angle and kernel row number ( $r_g = -0.39^+$ ). One likely reason for the lack of strong correlations might be the fact that there was not much variation for ear traits (see Table 2). Estimates of  $\sigma_g^2$  were not significantly different from zero for KD, CD, and CW. However, in general, there is a lot less variation in the ear architecture compared to tassel architecture, as the corn ear is very constrained, and it has been subjected to strong selection. To understand better the relations between the tassel and ear architecture components, further research has to be performed in other mapping populations and with a larger set of diverse lines that show considerable variation for both tassel and ear architecture components.



set of traits, we were able to detect QTL that might affect different stages of inflorescence development. One notable aspect of this research is the identification of QTL influencing the transition of various steps in inflorescence development. We identified QTL for the ratio total spikelets on central spike/branch number in bin 4.08 (Table 5), which explained 11.3% of  $\sigma_p^2$ , but we did not detect QTL for either total spikelets or branch number in this region. This QTL might influence only the transition from long BM to short BM or SPM. Similarly, we also identified QTL for the three tassel length ratios in regions that were not significant for either total tassel length or central spike length, even though they were used to calculate the ratios.

One important aspect concerning efficient use of QTL in marker-assisted selection is the congruency of positions of QTL across different populations. We compared our QTL results with previous studies by Berke and Rocheford (1999) in Illinois High Oil  $\times$  Illinois Low Oil  $F_1$  derived  $S_1$  population, and Mickelson et al (2002) in Mo17  $\times$  B73 recombinant inbreds, which studied a subset of tassel traits investigated here, as well as Veldboom and Lee (1994) that reported QTL for ear traits in Mo17  $\times$  H99  $F_{2:3}$  population. The criterion of overlapping bin regions used by Tuberosa et al (2002) was used to declare the QTL congruent between populations for a specific trait. We detected a QTL for tassel weight in bin 7.03 consistent with Berke and Rocheford (1999) and a QTL for cob diameter (the only common trait measured) in bin 1.07 consistent with Veldboom and Lee (1994). One of the reasons for finding few congruent QTL may

be due to the use of different parents and that epistasis might modulate the effect of a QTL depending on the genetic background. To overcome this bottleneck, we are evaluating a few mapping populations that have B73 as a parent, growing some in the same environments.

Many of the QTL appear to affect multiple traits and further research has to be done to learn whether there is a single gene with pleiotropic effect underlying the common QTL or there is a cluster of tightly linked genes. Of the 24 distinct QTL, 50% affected two or more traits and only some of these pairs of traits were supported by significant genotypic correlations. There was a significant correlation ( $r=0.6^{**}$ ) between the  $r_g$  values and the fraction of common QTL for all the traits (see Fig. 5a). However, when we investigated for traits directly measured on tassels and cobs, there was no significant correlation between the  $r_g$  and fraction of common QTL (see Fig. 5b). One of the reasons for not detecting common QTL for traits that were significantly correlated might be our models only explained a fraction of  $\sigma_g^2$ . In addition, we detected different sets of QTL for different traits due to sampling effects. It is possible that a number of small-effect QTL, which may be responsible for a large proportion of trait variation, are in common for those traits.

When we compared the  $r_g$  values with the fraction of common QTL for calculated traits with the traits used in their calculation, we found a significant correlation ( $r=0.7^*$ ). However, in some instances, we did not detect any common QTL for traits that had a high  $r_g$  value of 0.75. One of the reasons might be that the calculated

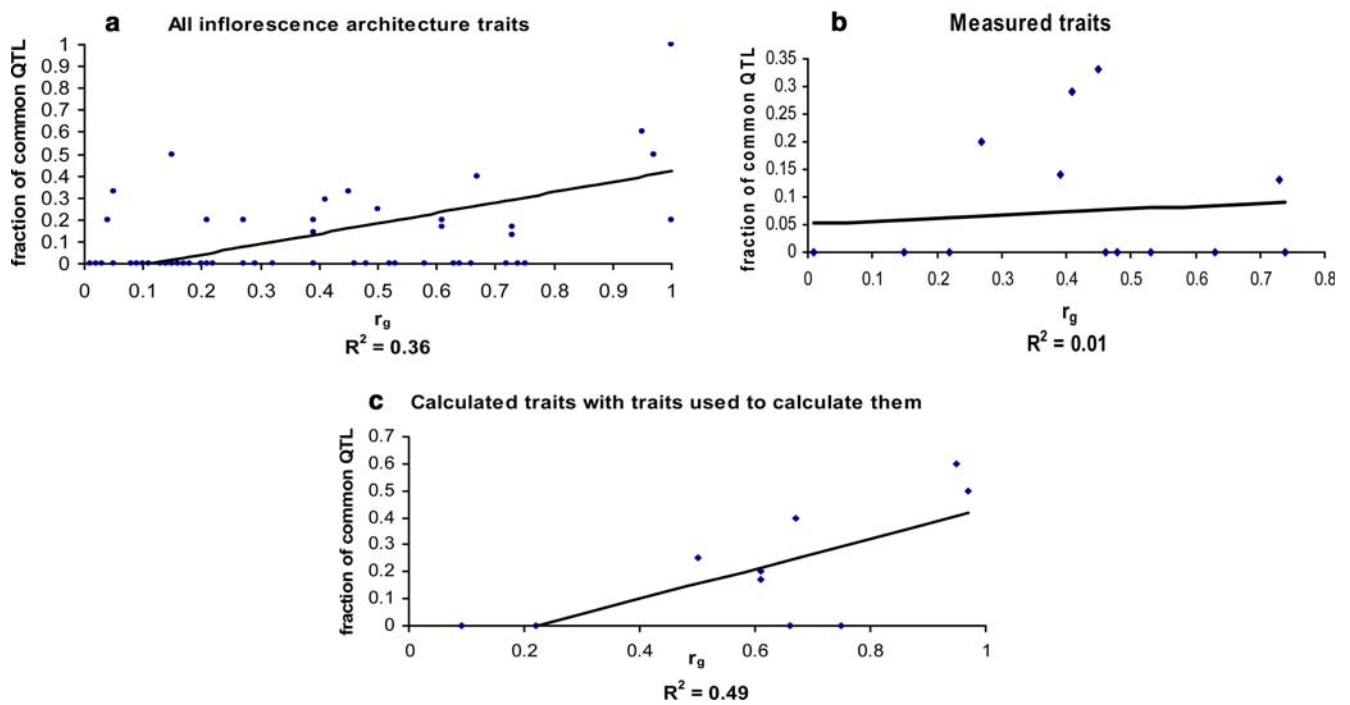


**Fig. 5** Plot of genotypic correlation coefficient ( $r_g$ ) and the fraction of common QTL for **a** all the traits that had significant  $\sigma_g^2$ , **b** the traits measured on the tassels and ears that had significant  $\sigma_g^2$ , and **c** calculated traits and traits used in their calculation

traits were distinct architectural traits and not merely linear functions of the measured traits and thus might have a different set of genes controlling them. These results support the validity of calculating ratios of measured traits in order to understand the genetic control of some complex steps in inflorescence development.

Some of the QTL are in chromosomal regions with known genes that affect tassel and ear development. We detected QTL for cob weight, tassel branch angle, and primary branch spikelet pair density in bin 5.04. A possible candidate gene in this region is *tdl*, which also maps to bin 5.04 and is known to increase the production of male and female SM. The QTL on chromosome 7 for branches and cob weight has *ral* as flanking marker. *Ramosal* mutants have many tassel branches (Neuffer et al. 1997), making it a logical candidate gene for branch number. Many of the inflorescence architectural genes have not yet been mapped on our population, but their bin numbers (taken from MaizeGDB) matched the bin numbers of QTL for traits known to be affected by those genes. For kernel number per row we detected a QTL ( $\sigma_p^2$  explained = 16.5%) in the same bin (3.02) as *ra2*. *Ramosa2* mutants, just like *ra1*, have excessive tassel branches and disorganized kernel rows in ears. A QTL for branch number was identified in the same bin (4.05) as *fea2* (MaizeGDB), which is known to initiate more branches.

We detected QTL for several traits in bins 6.07, 8.02, and 9.02, where no genes influencing inflorescence architecture have been mapped, perhaps due to redundancy, an essential role in viability, or simply because a mutant allele has not been found yet. This indicates our QTL analysis approach is revealing new chromosome regions with additional genes controlling inflorescence architecture, and is thus serving in the initial stages of gene discovery.

**Acknowledgments** This research was supported by NSF Plant Genome Research Program Grant 0110189 on Regulation of Inflorescence Architecture of Maize. We thank E. Vollbrecht and R. Martienssen for sharing *ral* sequence and P. Bommert and W. Weir for sharing *tdl* sequence. We appreciate technical assistance of Jerry Chandler and Don Roberts.

## References

- Austin DF, Lee M (1996) Comparative mapping in  $F_{2,3}$  and  $F_{6,7}$  generations of quantitative trait loci for grain yield and yield components in maize. *Theor Appl Genet* 92:817–826
- Austin DF, Lee M, Veldboom LR, Hallauer AR (2000) Genetic mapping in maize with hybrid progeny across testers and generations: grain yield and grain moisture. *Crop Sci* 40:30–39
- Beavis WD, Smith OS, Grant D, Fincher R (1994) Identification of quantitative trait loci using a small sample of topcrossed and  $F_4$  progeny from maize. *Crop Sci* 34:882–896
- Berke TG, Rocheford TR (1995) Quantitative trait loci for flowering, plant and ear height, and kernel traits in maize. *Crop Sci* 35:1542–1549
- Berke TG, Rocheford TR (1999) Quantitative trait loci for tassel traits in maize. *Crop Sci* 39:1439–1443
- Bommert P, Lunde C, Nardmann J, Vollbrecht E, Running M, Jackson D, Hake S, Werr W (2005a) Thick tassel dwarf1 encodes a putative maize ortholog of the Arabidopsis CLAVATA1 leucine-rich repeat receptor-like kinase. *Development* 132:1235–1245
- Bommert P, Satoh-Nagasawa N, Jackson D, Hirano H (2005b) Genetics and evolution of inflorescence and flower development in grasses. *Plant Cell Physiol* 46(1):69–78
- Churchill GA, Doerge RW (1994) Empirical threshold values for quantitative trait mapping. *Genetics* 138:963–971
- Cortez-Mendoza H, Hallauer AR (1979) Divergent mass selection for ear length in maize. *Crop Sci* 19:175–178
- Draper RW, Smith H (1981) Applied regression analysis, 2nd edn. Wiley, New York, p 307
- Dudley JW (1994) Molecular markers in plant improvement—manipulation of genes affecting quantitative traits (vol 33, p 663, 1993). *Crop Sci* 34:322
- Duvick DN, Cassman KG (1999) Post-green revolution trends in yield potential of temperate maize in the North-Central United States. *Crop Sci* 39:1622–1630
- Falconer DS (1989) Introduction to quantitative genetics, 3rd edn. Longman Scientific & Technical, New York
- Federer WT, Wolfinger RD (1998) SAS code for recovering intereffect information in experiments with incomplete blocks and lattice rectangle designs. *Agron J* 95:545–551
- Fischer KS, Edmeades GO, Johnson EC (1987) Recurrent selection for reduced tassel branch number and reduced leaf area density above the ear in tropical maize populations. *Crop Sci* 27:1150–1156
- Geraldi IO, Miranda Filho JB, Vencovsky R (1985) Estimates of genetic parameters for tassel characters in maize (*Zea mays* L) and breeding perspectives. *Maydica* 30:1–14
- Goldman IL, Rocheford TR, Dudley JW (1993) Quantitative trait loci influencing protein and starch concentration in the Illinois long term selection maize strains. *Theor Appl Genet* 87:217–224
- Haley CS, Knott SA (1992) A simple regression method for mapping quantitative trait loci in line crosses using flanking markers. *Heredity* 69:315–324
- Hallauer AR, Miranda JB (1988) Quantitative genetics in maize breeding. Iowa State University Press, Ames
- Hallauer AR, Ross AJ, Lee M (2004) Long-term divergent selection for ear length in maize. *Plant Breed Rev* 24(2):153–168
- Hospital F, Moreau L, Lacoudre F, Charcosset A, Gallias A (1997) More on the efficiency of marker assisted selection. *Theor Appl Genet* 95:1181–1189
- Jansen RC, Stam P (1994) High resolution of quantitative traits into multiple loci via interval mapping. *Genetics* 136:1447–1455
- Kaplinsky NJ, Freeling M (2003) Combinatorial control of meristem identity in maize inflorescence. *Development* 130:1149–1158
- Knapp SJ, Stroup WW, Ross WM (1985) Exact confidence intervals for heritability on a progeny mean basis. *Crop Sci* 25:192–194
- Lambert RJ, Johnson RR (1977) Leaf angle, tassel morphology, and the performance of maize hybrids. *Crop Sci* 18:499–502
- Lopez-Reynoso JJ, Hallauer AR (1998) Twenty-seven cycles of divergent mass selection for ear length in maize. *Crop Sci* 38:1099–1107
- MaizeGDB, the community database for maize genetics and genomics (2004) <http://www.maizegdb.org/>; verified 25 May 2005
- McSteen P, Hake S (2001) *Barren inflorescence2* regulates axillary meristem development in the maize inflorescence. *Development* 128:2881–2891
- Mickelson SM, Stuber CS, Senior L, Kaeppeler SM (2002) Quantitative trait loci controlling leaf and tassel traits in a B73 × Mo17 population of maize. *Crop Sci* 42:1902–1909
- Mikkilineni V (1997) Restriction fragment length polymorphism analysis of the Illinois long-term selection chemical strains. University of Illinois, Urbana
- Mode CJ, Robinson HF (1959) Pleiotropism and genetic variance and covariance. *Biometrics* 15:518–537

- Neuffer MG, Coe E, Wessler SR (1997) The mutants of maize. Cold Spring Harbor Lab Press, New York
- Odhiambo MO, Compton WA (1987) Twenty cycles of divergent mass selection for seed size in corn. *Crop Sci* 27:1113–1116
- Panzea database (2005) <http://www.panzea.org/>; verified 25 March 2005
- Robertson DS (1985) A possible technique for isolating genic DNA for quantitative traits in plants. *J Theor Biol* 117:1–10
- Robinson HF, Comstock RE, Harvey PH (1951) Genotypic and phenotypic correlations in corn and their implications in selection. *Agron J* 43:282–287
- Salazar MA, Hallauer AR (1986) Divergent mass selection for ear length in maize. *Braz J Genet* 9:281–294
- SAS Institute (2003) SAS proprietary software release 9.1. SAS Institute Inc, Cary
- Senior ML, Chin ECL, Lee M, Smith JSC, Stuber CW (1996) Simple sequence repeat markers developed from maize sequences found in the GENBANK database: map construction. *Crop Sci* 36:1676–1683
- Taguchi-Shiobara F, Yuan Z, Hake S, Jackson D (2001) The *fasciated ear2* gene encodes a leucine-rich repeat receptor-like protein that regulates shoot meristem proliferation in maize. *Genes Dev* 15:2755–2766
- Tuberosa R, Sanguineti MC, Landi P, Giuliani MM, Salvi S, Conti S (2002) Identification of QTLs for root characteristics in maize grown in hydroponics and analysis of their overlap with QTLs for grain yield in the field at two water regimes. *Plant Mol Biol* 48:697–712
- Utz HF (2001) PLABSTAT: a computer program for statistical analysis of plant breeding experiments. <http://www.uni-hohenheim.de/~ipspwww/soft.html>; verified 25 May 2005
- Utz HF, Melchinger AE (1996) PLABQTL: a program for composite interval mapping of QTL. <http://www.uni-hohenheim.de/~ipspwww/soft.html>; verified 25 May 2005
- Van Ooijen JW, Voorrips RE (2001) JoinMap 3.0, Software for the calculation of genetic linkage maps. Plant Research International, Wageningen, the Netherlands
- Veit B, Schmidt RJ, Hake S, Yanosfsky MF (1993) Maize floral development: new genes and old mutants. *Plant Cell* 5:1205–1215
- Veldboom LR, Lee M (1994) Molecular-marker-facilitated studies of morphological traits in maize II Determination of QTLs for grain yield and yield components. *Theor Appl Genet* 89:451–458
- Veldboom LR, Lee M (1996) Genetic mapping of quantitative trait loci in maize in stress and nonstress Environments: I Grain yield and yield components. *Crop Sci* 36:1310–1319
- Vollbrecht E, Springer P, Buckler E, Goh L, Martienssen RA (2005) Architecture of floral branch systems in maize and related grasses. *Nature* 436:1119–1126
- Wong JC, Lambert RJ, Yaakov T, Rocheford TR (2003) QTL associated with accumulation of tocopherols in maize. *Crop Sci* 43:2257–2266
- Zeng ZB (1994) Precision mapping of quantitative trait loci. *Genetics* 136:1457–1468